

Connections Between Lattice Gauge Theory and Chiral Perturbation Theory

Maarten Golterman

Department of Physics, Washington University, St. Louis, MO 63130, USA
e-mail: maarten@aapje.wustl.edu

Abstract. In this talk, I address the comparison between results from lattice QCD computations and Chiral Perturbation Theory (ChPT). I briefly discuss how ChPT can be adapted to the much-used quenched approximation and what it tells us about the special role of the η' in the quenched theory. I then review lattice results for some quantities (the pion mass, pion scattering lengths and the $K^+ \rightarrow \pi^+ \pi^0$ matrix element) and what quenched ChPT has to say about them.

1 Introduction

Chiral Perturbation Theory (ChPT) (Weinberg (1979), Gasser and Leutwyler (1985), Gasser (1997)) gives us information about the functional dependence of quantities associated with low-energy Goldstone Boson (GB) physics on the light-quark masses. Examples of such quantities are the GB masses, decay constants and scattering amplitudes. At any given order, these relations between physical quantities and quark masses involve a finite number of constants (the “low-energy constants (LECs),” which cannot be determined from ChPT alone. Therefore, ChPT is predictive (at any given order) if we consider a number of physical quantities larger than the number of LECs needed at that order. These LECs can in principle be determined either by comparison with experimental data, or by a theoretical calculation from the underlying theory, the Standard Model.

The strong-interaction part of such calculations is nonperturbative, and this is where Lattice QCD (LQCD) comes in. In LQCD, physical quantities (or related quantities, such as weak matrix elements) are computed from first principles as a function of the quark masses. By fitting the results with the relations predicted by ChPT, one can then, in principle, determine the LECs. This is very similar to determining these constants from experimental data, with the added advantage that in LQCD one can vary the quark masses.

Of course, in general, LQCD results will need to be of a high precision in order to extract the $O(p^4)$ LECs, because, in general, they show up in the one-loop corrections to the tree-level predictions from ChPT. This means good control over both statistical and systematic errors in the lattice computations. For instance, we need the volume L^3 in lattice units to be large in order to use a small lattice spacing a , while keeping the physical volume large enough to fit the hadronic system of interest. It is important to keep in mind that lattice results

need to be extrapolated to the continuum limit before they can be compared with ChPT. Also, for ChPT to be valid, GB masses need to be small compared to the chiral symmetry breaking scale. Again, this leads to the requirement of large enough volumes. (Finite volume effects can be studied within ChPT (Gasser and Leutwyler (1987)); we will see some examples in the following. However, LQCD practitioners are not only interested in the comparison with ChPT!) The temporal extent of the lattice needs to be large enough so that the lowest state in any channel can be reliably projected out by taking the large-time limit of euclidean correlation functions.

This has led to the widespread use of the *Quenched Approximation* (QA) (Parisi et al. (1981), Weingarten (1982)), in which the quark determinant is omitted from the LQCD path-integral. This is equivalent to omitting all contributions to correlation functions that involve sea-quark loops (valence-quark loops resulting from contractions of quarks in composite operators of course remain present, as they have nothing to do with the determinant). The reason is that, if the fermion determinant is included, the necessary computer time increases by orders of magnitude if we keep the physical parameters (lattice spacing, volume, quark masses) the same.

Quenched QCD is a different theory from QCD (as we will see, it's not even a healthy theory!), and therefore the predictions of ChPT do not apply to lattice results obtained in the QA. Fortunately, it turns out that a quenched version of ChPT (QChPT) can be developed systematically, and it is in this framework that we can compare quenched LQCD with ChPT. Unfortunately, this also implies that the LECs predicted by quenched QCD are not necessarily equal to those of full QCD, and as such, knowledge of them is of somewhat limited value. In this talk, I will describe how QChPT works, and discuss some examples of the comparison of lattice results with ChPT. I should note right away that, as we will see, currently lattice data are not precise enough yet to unambiguously see ChPT one-loop effects.

Before we get into this, let me end this introduction with a few remarks. First, recently, more lattice results with “dynamical fermions” (i.e. including sea-quark loops) are becoming available. However, since the overhead in computing the fermion determinant is so large, these results are often for one or two values of the sea-quark mass, while many values of the valence quark masses are considered. The methods described in this talk can easily be adapted to these “partially quenched” theories with sea quarks with a mass that differs from that of the valence quarks (Bernard and Golterman (1994), Sharpe (1997b)). Second, the study of QChPT sheds much light on the nature of the QA, and, as such, has been very helpful for LQCD.

2 Quenched ChPT, the η' , and the Pion Mass

Euclidean quenched QCD can be defined by taking the ordinary QCD lagrangian, and adding a new set of quarks $\{\tilde{q}_i\}$ to it which carry one-by-one exactly the

same quantum numbers as the normal quarks $\{q_i\}$, but which have opposite statistics (Morel (1987)):

$$\mathcal{L} = \bar{q}_i(\not{D} + m_i)q_i + \bar{\tilde{q}}_i(\not{D} + m_i)\tilde{q}_i, \quad i = u, d, s. \quad (1)$$

We will refer to these new wrong-statistics quarks as “ghost-quarks.” The reason for their introduction is that the contribution coming from integrating over these ghost-quarks exactly cancels the determinant which comes from the integration over the normal quarks. It is easy to see this diagrammatically: while a minus sign is needed for every occurrence of a quark loop, this is not the case for a ghost-quark loop, because of their bosonic statistics. So, for every diagram with a quark loop, a similar diagram contributes with that one loop replaced by a ghost-quark loop, therefore leading to the cancellation of this diagram.

For $m_i = 0$, the lagrangian (1) is invariant under a *six*-flavor chiral symmetry group (Bernard and Golterman (1992)). A typical transformation looks like

$$\begin{pmatrix} q'_i \\ \tilde{q}'_i \end{pmatrix} = \begin{pmatrix} A_{ij} & B_{ij} \\ C_{ij} & D_{ij} \end{pmatrix} \begin{pmatrix} q_j \\ \tilde{q}_j \end{pmatrix}, \quad (2)$$

where A , B , C and D are 3×3 blocks, with B and C containing anticommuting numbers, since they transform bosons into fermions and vice versa. This group is known as a *graded* version of $U(6)$, and is denoted by $U(3|3)$. For $m_i = 0$, the symmetry of (1) is therefore $U(3|3)_L \times U(3|3)_R$.

We will assume that gluons are responsible for forming mesonic bound states. In this case, since gluons couple equally to quarks and ghost-quarks, that means that not only the usual $q\bar{q}$ GBs (i.e. π , K , η and η') will occur, but also $q\bar{\tilde{q}}$ “ghost-mesons,” and $q\tilde{\bar{q}}$, $\tilde{q}\bar{q}$ *fermionic* “hybrid” mesons. (For the role of η' , see below.) QChPT can then be developed systematically in a way completely analogous to the usual three-flavor case (Bernard and Golterman (1992), for other early work on QChPT, see Sharpe (1990,1992)), but now for the group $U(3|3)_L \times U(3|3)_R$. The quenched effective lagrangian describes the low-energy physics of all Goldstone mesons, ghosts and fermionic hybrids included.

Lack of space prevents me from giving more details on the technicalities of QChPT (see e.g. Golterman (1994)). However, before we continue to consider any examples, we need to address the very special role of the η' . In unquenched QCD, the η' is not a GB because of the $U(1)_A$ anomaly. In quenched QCD, we would expect that a similar role is played by some linear combination of η' and $\tilde{\eta}'$. We can understand which linear combination by realizing that ghost-quark loops do *not* contribute a minus sign, so that we get a nonzero triangle anomaly between the $U(1)$ axial current and two gluons by *subtracting* the triangle graphs with a ghost-quark running around the loop from those with normal quarks. Hence in the quenched theory, the “anomalous” meson is the “super- η' ”, $(\eta' - \tilde{\eta}')/\sqrt{2}$. The super- η' transforms as a singlet under the nonanomalous part of the graded chiral symmetry group, and therefore arbitrary functions of this field (and its derivatives) appear in the effective lagrangian (Gasser and Leutwyler (1985), Bernard and Golterman (1992)).

Let us consider the lowest order, $O(p^2)$ part of the effective lagrangian quadratic in the η' and $\tilde{\eta}'$ fields:

$$\begin{aligned} \mathcal{L}_{\eta'} = & \frac{1}{2}(\partial_\mu \eta')^2 - \frac{1}{2}(\partial_\mu \tilde{\eta}')^2 + \frac{1}{2}m_\pi^2(\eta'^2 - \tilde{\eta}'^2) \\ & + \frac{1}{2}\mu^2(\eta' - \tilde{\eta}')^2 + \frac{1}{2}\alpha(\partial_\mu(\eta' - \tilde{\eta}'))^2, \end{aligned} \quad (3)$$

where the terms on the second line are the quadratic, $O(p^0)$ and $O(p^2)$ parts of the arbitrary functions of the super- η' field. All minus signs originate from the graded nature of the chiral symmetry group (in building invariants for such a group, the supertrace plays the role of the trace in the ordinary case, see DeWitt (1984)). They will have important consequences. For simplicity we assumed degenerate quark masses.

If we omit the $\tilde{\eta}'$ field from (3), we obtain the quadratic part of $\mathcal{L}_{\eta'}$ for the unquenched theory, and the parameter μ^2 would essentially be the singlet part of the η' mass (one can show that μ^2 does not vanish because of the anomaly!). So, let us see what happens in the quenched case. We will treat the first line in (3) as the part defining η' and $\tilde{\eta}'$ propagators $S_{\eta'}^0(p)$ and $S_{\tilde{\eta}'}^0(p)$:

$$S_{\eta'}^0(p) = -S_{\tilde{\eta}'}^0(p) = \frac{1}{p^2 + m_\pi^2}. \quad (4)$$

The second line defines the two-point vertices $-(\mu^2 + \alpha p^2)$ for η' - η' , $\tilde{\eta}'$ - $\tilde{\eta}'$ and for η' - $\tilde{\eta}'$ mixing. We can find the complete η' two-point function by summing all diagrams containing an arbitrary number of these two-point vertices on an η' line (taking into account combinatoric factors):

$$\begin{aligned} S_{\eta'}(p) = & S_{\eta'}^0(p) \\ & - S_{\eta'}^0(p)(\mu^2 + \alpha p^2)S_{\eta'}^0(p) \\ & + S_{\eta'}^0(p)(\mu^2 + \alpha p^2)(S_{\eta'}^0(p) + S_{\tilde{\eta}'}^0(p))(\mu^2 + \alpha p^2)S_{\eta'}^0(p) \\ & - \dots \end{aligned} \quad (5)$$

Using (4), we see that the third line in (5) vanishes (and so do all higher order contributions), leading to

$$S_{\eta'}(p) = \frac{1}{p^2 + m_\pi^2} - \frac{\mu^2 + \alpha p^2}{(p^2 + m_\pi^2)^2}. \quad (6)$$

It is actually easy to convince oneself, that this cancellation is nothing else than the cancellation of sea-quark loops with their ghost counterparts. The vertex $-(\mu^2 + \alpha p^2)$ represents the annihilation of the valence quark antiquark pair in the η' (which is a flavor singlet, making this annihilation possible), and the creation of either a quark antiquark, or a ghost-quark ghost-antiquark pair. Tracing the quark flow for each of the terms in (5), one finds that quark and ghost-quark loops occur for all terms with more than one vertex insertion.

From (6), it is clear that the η' is “sick” in the QA because there is no particle interpretation for the double pole term. Moreover, it tells us that we *have to keep* the η' in the QA, because it has poles which are degenerate with those of the other Goldstone mesons. These poles can lead to chiral logarithms that have no counterpart in the unquenched theory. In the case of nondegenerate quark masses, the π^0 and η will inherit the problems of the η' through mixing.

As an example, consider the one-loop expression for the pion mass in terms of the quark mass, calculated in QChPT:

$$m_\pi^2 = Am_q(1 + \delta \log Bm_q + Cm_q), \quad (7)$$

$$\delta = \frac{\mu^2}{24\pi^2 f_\pi^2}, \quad (8)$$

where, for simplicity, we set $\alpha = 0$ (of course in comparing with real data, one has to take α into account). A , B and C are parameters related to the LECs, which are not predicted by ChPT. We see that the chiral log in (7) is entirely due to the double pole term in the η' propagator (because it is proportional to μ^2). In unquenched ChPT, the chiral log would be multiplied by an extra factor m_q , and be more suppressed for small quark mass. In fact, in the quenched case, the quantity m_π^2/m_q diverges in the chiral limit, $m_q \rightarrow 0$! This is the first example of the highly infrared divergent behavior of quenched QCD. (I believe that this divergence is a sickness of quenched QCD, and not just of QChPT (Bernard and Golterman (1993)).)

In Fig. 1, I show lattice results for this quantity (in lattice units), from a compilation of staggered fermion spectrum results by Gottlieb (1997) (see this review for the original refs. on all these data). The mass ratio on the horizontal axis is basically the quark mass. $\beta = 5.7$ corresponds to a lattice spacing $a \approx 0.2$ fm, while $\beta = 6.5$ corresponds to $a \approx 0.055$ fm. The squares and fancy crosses correspond to the data with the largest spatial volumes. The overlapping squares have $L \approx 2.6$ fm and $L \approx 3.5$ fm, while the highest square (for lowest quark mass) has $L \approx 1.8$ fm. The fancy crosses have $L \approx 2.6$ fm. The fact that the squares for $L \approx 2.6$ fm and $L \approx 3.5$ fm overlap indicates that $L \approx 2.6$ fm is large enough to not have finite volume effects larger than the size of the error bars. Points for different β do not fall onto one curve because the quantity on the vertical axis depends on a . While the data do show an upward trend with decreasing quark mass, as predicted by (7), we cannot conclude that this behavior is unambiguously seen in these data. We know that scaling violations occur for the data at the two lower β values, so that these cannot be reliably compared to the continuum prediction of QChPT. At larger β , the curves look flatter, and more data for small quark masses at these higher values of β will be needed to fit (7). Qualitatively, we do see a departure from the ChPT tree-level prediction $m_\pi^2 \propto m_q$, which would correspond to a horizontal line in Fig. 1. For a recent, much more detailed discussion of attempts to fit (7) to lattice data, including a list of subtleties and pitfalls, see Sharpe (1997a). We note here that it is probably better to determine δ from a certain ratio of decay constants (Bernard and Golterman (1993), Bhattacharya and Gupta (1996), Sharpe (1997a)).

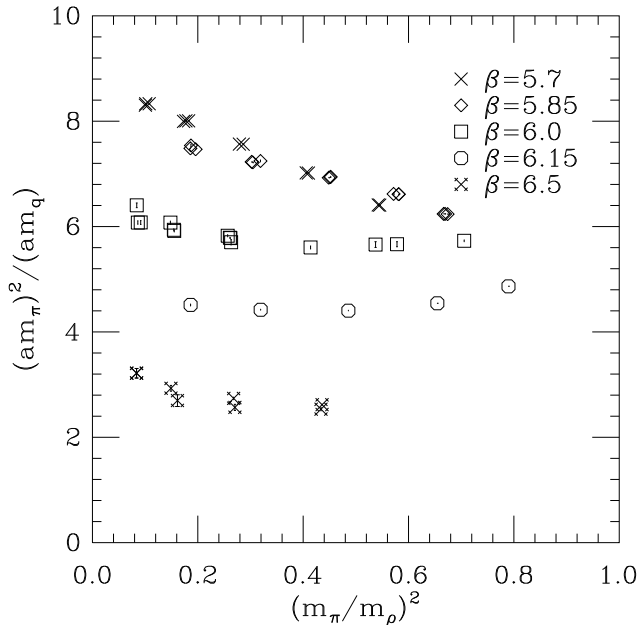


Fig. 1. Quenched staggered fermion lattice results for m_π^2/m_q , in lattice units, versus the quark mass in dimensionless units (see text). From the Lattice 96 spectrum review (Gottlieb (1997)).

The logarithm in (7) appears with the coefficient δ , instead of the usual $m_\pi^2/(4\pi f_\pi)^2$, and therefore is of the same order as the tree-level term in chiral power counting. At more than one loop, there are contributions of the same order in $m_\pi^2/(4\pi f_\pi)^2$, but higher order in δ . This means that, in order for QChPT to be systematic, δ has to be treated as a small parameter. In unquenched QCD, we can estimate δ from the η' mass, yielding $\delta \approx 0.18$. Of course, since the quenched theory is different, δ could have a different value in this case, and it is important to determine its value numerically. It is believed that the quenched value does not differ much from the unquenched value, but errors are not yet sufficiently under control to quote a number (Sharpe (1997a)). We also note here that both μ^2 and α are of order $1/N$ in the large- N expansion (Veneziano (1979), Witten (1979)).

There is an extensive body of work on QChPT, and I do not have space here to properly review even a substantial fraction of it. There has been work on the inclusion of other hadrons (baryons: Labrenz and Sharpe (1996), vector and tensor mesons: Booth et al. (1997), Chow and Rey (1997), heavy baryons: Chiladze

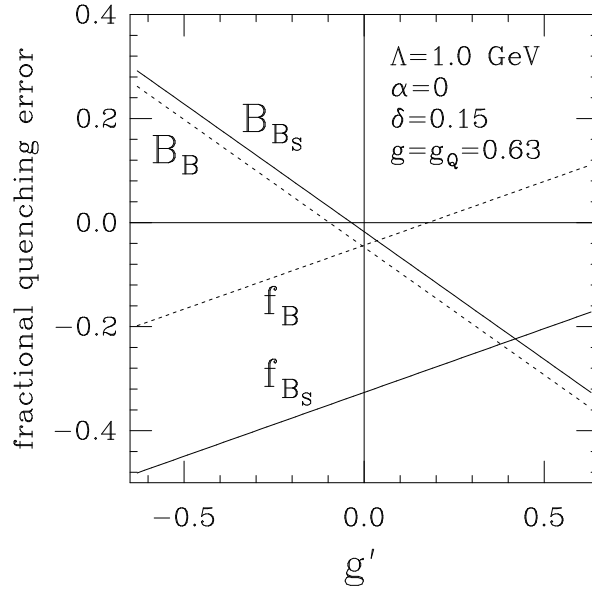


Fig. 2. Relative error from quenching in f_B , f_{B_s} , B_B and B_{B_s} at one-loop in QChPT. For explanation and assumptions, see text. From Sharpe and Zhang (1996).

(1997)), weak matrix elements (B_K : Sharpe (1992), f_B and B_B : Booth et al. (1995), Sharpe and Zhang (1996), $K^+ \rightarrow \pi^+\pi^0$ and B_K : Golterman and Leung (1997), baryon axial charge: Kim and Kim (1996)), pion scattering (Bernard and Golterman (1996)) and formalism (Colangelo and Pallante (1997)). For work on fitting lattice data to results from QChPT, I refer to the Proceedings of the Lattice 96 and Lattice 97 conferences, in particular the reviews by Gottlieb (1997), Sharpe (1997a) and Yoshie (1997), and references therein.

Here, let me show a sample result of a case where the GBs are coupled to other hadrons, in this case the B meson. Fig. 2, taken from Sharpe and Zhang (1996), shows the relative error from quenching for f_B , f_{B_s} , B_B and B_{B_s} , as a function of the many parameters that are not determined by ChPT, from a one-loop ChPT calculation. Note that more parameters typically show up than in the case of pure GB physics, because of the various coupling constants between the GBs and the heavy sector. g (g_Q) is the B -pion coupling in the unquenched (quenched) theory, g' is the B - η' coupling (which is suppressed in $1/N$). The figure assumes $g_Q = g$, and values as shown (the value for g is from an estimate in the unquenched theory). All $O(p^4)$ LECs have arbitrarily been set to zero, while the cutoff is chosen at $\Lambda = 1$ GeV. Fig. 2 shows that, under these assumptions, quenching errors in these quantities can be large. As such, it gives

us useful information, but it should be stressed that this is *not* a calculation of quenching errors, because of the many possibly unjustified choices made for all the parameters. This situation is typical in the case that we consider the effective theory for GBs coupled to other hadrons.

3 Pion Scattering

LQCD computations give us access to euclidean correlation functions only, and, lacking the possibility to analytically continue them to Minkowski space, it appears impossible to extract information on scattering lengths from the lattice. However, we can make use of the fact that lattice computations are necessarily done in a finite volume, and use this as a probe of the interactions between two pions. More precisely, one can compute the energy of a state with two pions at rest from the euclidean correlation function (for $I = 2$, a similar correlation function can be defined for $I = 0$)

$$\begin{aligned} C_{I=2} &= \langle 0 | \pi^+(t) \pi^+(t) \pi^-(0) \pi^-(0) | 0 \rangle \\ &= \sum_{|\alpha\rangle} e^{-E_\alpha t} |\langle \alpha | \pi^-(0) \pi^-(0) | 0 \rangle|^2 \\ &= Z e^{-2m_\pi t} (1 - \Delta E t + O(t^2)) + \text{excited states}, \end{aligned} \tag{9}$$

where $\pi^-(0)$ creates a zero-momentum π^+ at time 0, and $\pi^+(t)$ annihilates a zero-momentum π^+ at time t . We inserted a complete set of states $\{|\alpha\rangle\}$, and assume that we can take t large enough to project out the lowest-energy state. This is the state with two pions at rest in finite volume, with $E_{2\pi} = 2m_\pi + \Delta E$, where ΔE is the energy shift due to finite volume effects (in infinite volume, two pions at rest do not interact). We expanded in $\Delta E t$, because it is in this form that the energy shift will show up in a ChPT calculation. Also, it was this form which has been fitted to lattice data by various groups in attempts to determine ΔE (Guagnelli et al. (1990), Gupta et al. (1992), Kuramashi et al. (1993)). From (9) we see that $\Delta E t$ has to be small enough for the expansion on the last line to be valid (but of course t has to be large enough to project out the excited states).

As mentioned above, ΔE is a measure of the interactions between the two pions, due to their confinement to a finite volume. A precise connection between ΔE and the pion scattering length was given by Lüscher (1986):

$$\Delta E = -\frac{4\pi a_0}{m_\pi L^3} \left(1 - 2.837297 \frac{a_0}{L} + 6.375183 \frac{a_0^2}{L^2} \right) + O\left(\frac{1}{L^6}\right), \tag{10}$$

where a_0 is the infinite volume scattering length for the corresponding channel ($I = 0$ or 2). While the proof of (10) is more general, the r.h.s. can be recovered term by term at tree level, one loop, two loops, etc. in ChPT. It is instructive to look at this in some detail, because it will tell us how things change in the QA.

Consider the one-loop diagram in which the pions are created at time 0, scatter at time $t_2 > 0$, rescatter at time $t_1 > t_2$, and then are annihilated at time $t > t_1$. (There are many other one-loop contributions of course, but it is this one that leads to the $1/L^4$ term in (10).) Since the initial and final pions have zero spatial momentum, their propagators are of the form $\exp(-m_\pi t)$ if they “travel” a time t ; the expression for this diagram looks like

$$\lambda^2 L^3 e^{-2m_\pi t} \frac{1}{L^3} \sum_{\mathbf{k}} e^{-2(E(\mathbf{k})-m_\pi)(t_1-t_2)}, \quad E(\mathbf{k}) = \sqrt{m_\pi^2 + \mathbf{k}^2}. \quad (11)$$

The second exponential takes into account that between the two scatterings, the two pions can have arbitrary momenta \mathbf{k} and $-\mathbf{k}$. The overall factor L^3 comes from integrating the diagram over the spatial volume, and $\lambda \propto m_\pi^2/(4\pi f_\pi)^2$ is the interaction strength. This expression has to be integrated over t_1 and t_2 , where here we are interested in the contribution with $0 < t_2 < t_1 < t$. This integration leads to

$$t \frac{1}{L^3} \sum_{\mathbf{k} \neq 0} \frac{1}{E(\mathbf{k}) - m_\pi} \quad (12)$$

(the $\mathbf{k} = 0$ term contributes to the $O(t^2)$ term in (9)). In infinite volume, we may replace $\frac{1}{L^3} \sum_{\mathbf{k} \neq 0}$ by $\int d^3k$, and (after renormalization) we get a contribution $\sim \lambda^2/L^3$ to ΔE . (The L^3 in (11) turns into a $1/L^3$ after dividing by the factor L^6 which normalizes the contribution $L^6 \exp(-2m_\pi t)$ of two noninteracting pions.) This just gives us a one-loop correction to a_0 in the $1/L^3$ term in (10). In a finite volume, the smallest momenta $k \sim 1/L$ cause the sum to deviate from the integral most prominently. Expanding $E(\mathbf{k}) - m_\pi \sim 1/L^2$ (keeping track of the L dependence only), the sum (12) gives a contribution $\sim t/L$. This leads to an additional finite volume contribution to ΔE of order $\lambda^2/L^4 \sim a_0^2/L^4$, cf. the second term in (10).

We can now also see how quenching, and in particular, the special role of the η' , will change this result. In the $I = 0$ channel, the intermediate mesons in the diagram I just discussed can also be singlets, and the two-point vertex $-(\mu^2 + \alpha p^2)$ can appear on these internal lines. Let us consider the case of one such insertion at time t_X . The expression for the diagram is similar to (11), but now we have to integrate also over t_X ! Considering the contribution where $t_2 < t_X < t_1$, we pick up an extra factor $t_1 - t_2$ after doing the integral over t_X , and from the integration over t_1 and t_2 we now get

$$t \frac{1}{L^3} \sum_{\mathbf{k} \neq 0} \frac{1}{(E(\mathbf{k}) - m_\pi)^2}. \quad (13)$$

Going through the same argument as before, this leads to an extra factor L^2 in the finite-volume energy shift, i.e. a contribution $\sim \delta/L^2$ to ΔE , quite unlike the prediction of Lüscher’s formula! Even worse, if we insert the η' two-point vertex on *both* internal lines, we find another factor L^2 enhancement, and a one-loop contribution to ΔE of order $\delta^2/L^0 = \delta^2$. These “enhanced finite volume”

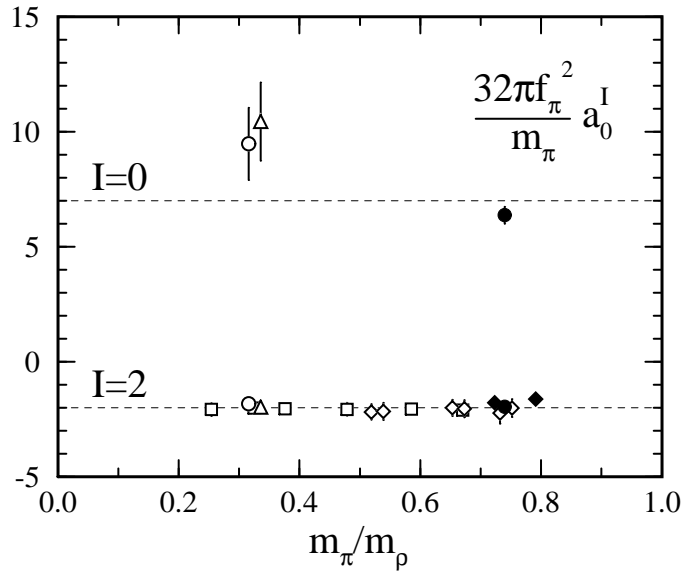


Fig. 3. Pion scattering lengths as a function of m_π/m_ρ . Errors are statistical only. The squares and diamonds are from Gupta et al. (1992), all other points are from Kuramashi et al. (1993), from which this figure was taken.

corrections are another example of the serious infrared problems that affect the quenched theory, due to the double pole in (6). For a complete analysis (and real calculation), see Bernard and Golterman (1996). We just note here that also the rest of the structure of (10) is not reproduced in the quenched theory. For $I = 2$ the problem is less serious, because no enhanced corrections occur (the internal lines cannot be singlets in this case).

We conclude that QChPT does not only break down for small L , but also for large L , since the tree-level term in ΔE goes like $1/L^3$, while there are one-loop corrections which go like a lower power of $1/L$. In fact, one has to worry whether QChPT applies for any choice of parameter values in this case! It is therefore very interesting to compare these results with quenched numerical computations of the pion scattering lengths.

In Fig. 3, which I took from Kuramashi et al. (1993), lattice results for $a_0^{I=0,2}$ are shown, in units of tree-level ChPT predictions, as a function of m_π/m_ρ . Also results from Gupta et al. (1992) for $I = 2$ are included (squares and diamonds). The volume is $12^3 \times 20$ in lattice units, $\beta = 5.7$, corresponding to $a \approx 0.2$ fm. We see that, within errors (only statistical errors are shown), the lattice results agree with ChPT at tree level. In Bernard and Golterman (1996) we considered the size of the one-loop QChPT corrections for the parameters of these lattice

computations, and found that they are always smaller than 20% of the tree-level values. However, we cannot directly compare the lattice results with ChPT because of the presence of other systematic errors, most notably scaling violations (a is too big), and contamination of excited states (t in (9) may not have been large enough to reliably project out the lowest state, see Bernard and Golterman (1996)).

4 $K^+ \rightarrow \pi^+\pi^0$ Decay

LQCD practitioners have had a long-standing interest in computing nonleptonic K -decay matrix elements, because of such prominent experimental observations as the $\Delta I = 1/2$ rule, and their importance in determining Standard Model parameters (the CKM-matrix). I will restrict myself here to $K^+ \rightarrow \pi^+\pi^0$. References Gavela et al. (1988), Bernard and Soni (1989) report on the status of past lattice computations of $\langle \pi^+\pi^0 | O_4 | K^+ \rangle$, while Ishizuka et al. (1997) reports on a very recent computation. Here $O_4 = (\bar{s}_L \gamma_\mu d_L)(\bar{u}_L \gamma^\mu u_L) + (\bar{s}_L \gamma_\mu u_L)(\bar{u}_L \gamma^\mu d_L) - (\bar{s}_L \gamma_\mu d_L)(\bar{d}_L \gamma^\mu d_L)$ is the $\Delta I = 3/2$, $\Delta S = 1$ component of the $SU(3)_L$ 27-plet responsible for this decay. In ChPT, we have, with Σ the nonlinear GB-field,

$$O_4 = \alpha_{27} t_{kl}^{ij} (\Sigma \partial_\mu \Sigma^\dagger)_i^k (\Sigma \partial^\mu \Sigma^\dagger)_j^l + O(p^4) \text{ operators}, \quad (14)$$

where t_{kl}^{ij} projects out the appropriate component, α_{27} is a free parameter, and the $O(p^4)$ operators were listed in Kambor et al. (1990). In Golterman and Leung (1997), $\langle \pi^+\pi^0 | O_4 | K^+ \rangle$ was calculated to one loop in order to compare the real world with lattice results. Since the $O(p^4)$ coefficients are not or very poorly known, we set them equal to zero, and estimated the error from this by considering two values of the cutoff $\Lambda = 770 \text{ MeV}/1 \text{ GeV}$. The real-world value then is (for tree level, see Donoghue et al. (1982), for one loop with $m_\pi = 0$, see Bijmans et al. (1984))

$$\langle \pi^+\pi^0 | O_4 | K^+ \rangle = \frac{12i\alpha_{27}}{\sqrt{2}f_\pi^3} (m_K^2 - m_\pi^2) \times \left(1 + \begin{array}{l} 0.63, \Lambda = 1 \text{ GeV} \\ 0.36, \Lambda = 770 \text{ MeV} \end{array} \right). \quad (15)$$

On the lattice, one computes the matrix element from

$$C(t_2, t_1) = \langle 0 | \pi^+(t_2) \pi^0(t_2) O_4(t_1) K^-(0) | 0 \rangle \quad (16)$$

$$\stackrel{t_2 \gg t_1 \gg 0}{\longrightarrow} e^{-E_{2\pi}(t_2-t_1)} e^{-m_K t_1}$$

$$\times \frac{\langle 0 | \pi^+(0) \pi^0(0) | \pi^+\pi^0 \rangle \langle \pi^+\pi^0 | O_4(0) | K^+ \rangle \langle K^+ | K^-(0) | 0 \rangle}{\langle \pi^+\pi^0 | \pi^+\pi^0 \rangle \langle K^+ | K^+ \rangle},$$

where all mesons are taken to be at rest. In actual lattice computations, degenerate quark masses were used, so that $m_K = m_\pi$. The matrix element in (16) therefore is not the one we want: it is unphysical because of the choice of masses and external momenta. Furthermore, there are power-like finite volume effects, and the QA has been used in all computations. All these systematic effects can

be estimated in one-loop ChPT (the unphysical choice of masses and momenta already at tree level in ChPT (Bernard and Soni (1989))).

To one loop in ChPT the physical matrix element and the unphysical quenched lattice matrix element (after extrapolation to the continuum limit) are related by (Golterman and Leung (1997))

$$\langle \pi^+ \pi^0 | O_4(0) | K^+ \rangle_{phys} = Y \frac{\alpha_{27}}{\alpha_{27}^q} \left(\frac{f_q}{f} \right)^3 \frac{m_K^2 - m_\pi^2}{2M_\pi^2} \langle \pi^+ \pi^0 | O_4(0) | K^+ \rangle_{unphys}^{quenched}, \quad (17)$$

with

$$Y = \frac{1 + \frac{0.089, \Lambda=1 \text{ GeV}}{-0.015, \Lambda=770 \text{ MeV}}}{1 + \frac{M_\pi^2}{(4\pi F_\pi)^2} \left[-3 \log \frac{M_\pi^2}{\Lambda_q^2} + F(M_\pi L) \right]}, \quad (18)$$

$$F(m_\pi L) = 17.827/(m_\pi L) + 12\pi^2/(m_\pi L)^3. \quad (19)$$

Here parameters with a subscript q are those of the quenched theory, and $M_\pi = M_K$, F_π refer to the lattice quantities. At tree level, we would have $Y = 1$. $O(p^4)$ LECs have been set to zero. Some remarks are in order:

- For degenerate quark masses, O_4 does not couple to the η' , which explains why (18) does not depend on δ and α . For nondegenerate quark masses, such dependence would show up, presumably making the QA less interesting in that case.
- The ratios $\alpha_{27}/\alpha_{27}^q$ and f_q/f are not known, and, in the following discussion of lattice results, we will arbitrarily set them equal to one.
- The $O(p^4)$ LECs are basically “absorbed” into the cutoff Λ . As before, we will take the cutoff equal to 770 MeV or 1 GeV *independently* in the quenched and unquenched theories, and take the spread as an indication of the systematic error associated with our lack of knowledge of these LECs.

In Fig. 4 I show lattice data for the matrix element from Bernard and Soni (1989) (open symbols), where the tree-level correction factor $(m_K^2 - m_\pi^2)/2M_\pi^2$ in (17) was already taken into account. The errors on these points are statistical only, and we left out points at pion masses with $M_\pi > m_\rho$ and/or at smaller volumes. The crosses show what we obtain if we “correct” the central values of each of these points with the factor Y (evaluated at the appropriate pion mass and volume). The errors on these points indicate the spread from choosing different combinations of Λ and Λ_q . We see that at all points $Y < 1$, and that therefore the one-loop corrections reduce the discrepancy between lattice data and the experimental result. However, since one-loop effects are rather substantial, two-loop effects can probably not be neglected. Also, again, scaling violations and various other systematic effects are not taken into account. For a more complete discussion, see Golterman and Leung (1997).

Very recently, the computation was done again by the JLQCD collaboration, with larger volumes, and larger β (Ishizuka et al. (1997)). The results are shown

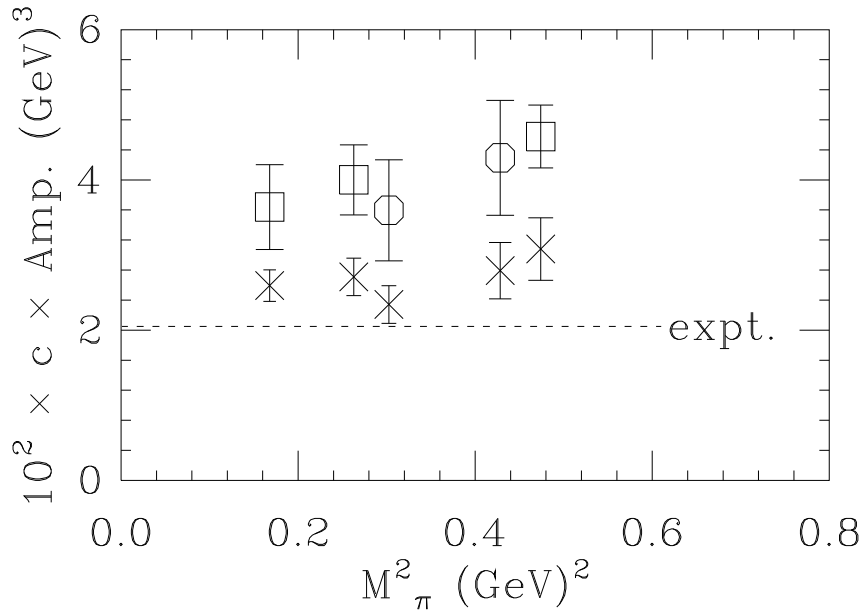


Fig. 4. $K^+ \rightarrow \pi^+\pi^0$ decay amplitude as a function of pion mass. Open symbols: data from Bernard and Soni (1989) (squares: $16^3 \times 25$ (or $\times 33$), $\beta = 5.7$; octagons: $24^3 \times 40$, $\beta = 6$); crosses: including the correction factor Y . The constant $c = 2\sqrt{2}/(G_F \sin \theta_c \cos \theta_c)$.

in Fig. 5 (without the one-loop correction factor Y , along with the data of Bernard and Soni (1989)) and Fig. 6 (with the factor Y taken into account). If the unquenched cutoff $\Lambda = \Lambda^{\text{cont}} = 1 \text{ GeV}$ is chosen, the values in Fig. 6 would come out about 10% higher. Again, I should stress that, because of the uncertainties in the estimates for Y , the lack of knowledge of the ratios $\alpha_{27}/\alpha_{27}^q$ and f_q/f , and various systematic effects which cannot be estimated in ChPT, one can only conclude that one-loop ChPT reduces the discrepancy between lattice and experiment.

5 Conclusion

It is clear that one-loop ChPT plays an important role in understanding current LQCD results. However, numerical computations are not yet at a level of precision that $O(p^4)$ LECs can be reliably extracted from the lattice. The most extensive (small quark masses, large volumes) computations are done in the (partially) QA, to which ChPT can be adapted systematically. The fundamen-

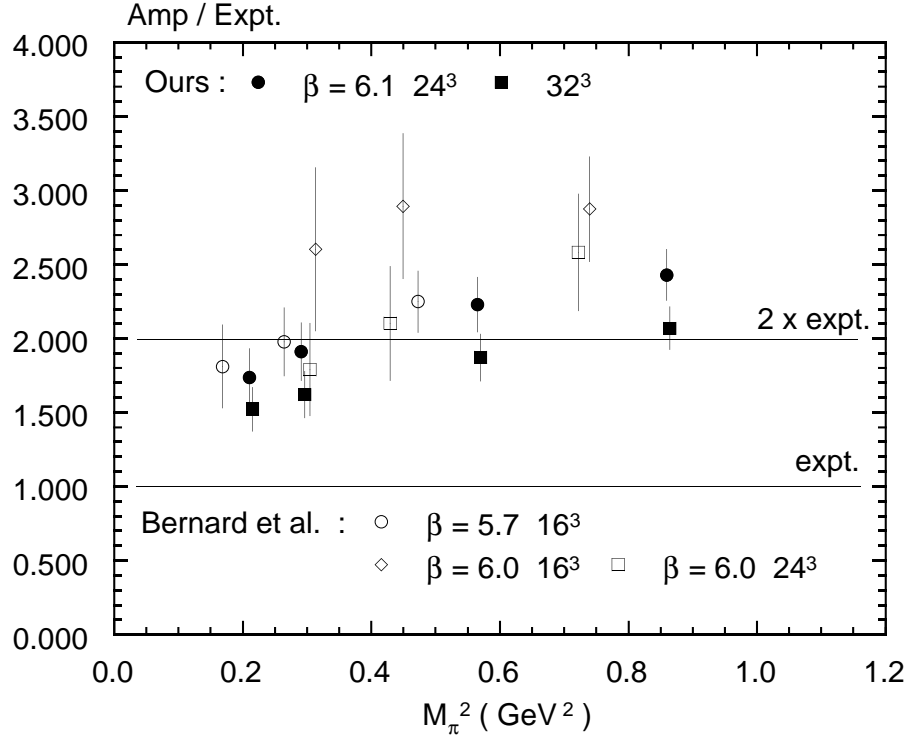


Fig. 5. $K^+ \rightarrow \pi^+\pi^0$ decay amplitude as a function of pion mass, in units of the experimental value. Figure provided by JLQCD (Ishizuka et al. (1997)). Also shown are the data from Bernard and Soni (1989). Tree-level corrected.

tal difference between QCD and its quenched relative shows up in full force at one-loop in ChPT: the nonanalytic terms in the QA are in general very different from those of the full theory. The safest way to look at these one-loop differences is to take them as an indication of the systematic error made by using the QA.

We have seen that the quenched theory is afflicted with infrared divergences which show up as a diverging chiral limit, and a diverging infinite volume limit. This is all due to the special role of the η' in the QA. It is therefore important to test the predictions of QChPT against lattice computations, as long as we will be using the (partially) QA.

Acknowledgements. I would like to thank the organizers and participants of the Workshop for creating a stimulating atmosphere. I would also like to thank Claude Bernard, Steve Gottlieb, Naruhito Ishizuka, Ka Chun Leung, Steve Sharpe and Akira Ukawa for many discussions on various aspects of the work described here and for providing me with the figures, and Pierre van Baal and

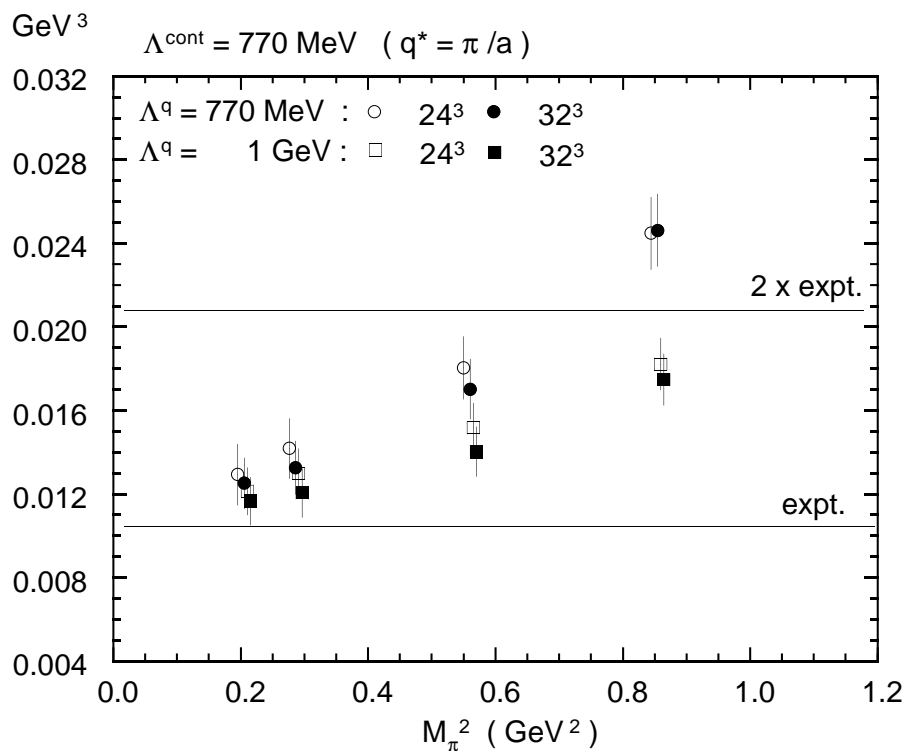


Fig. 6. $K^+ \rightarrow \pi^+\pi^0$ decay amplitude as a function of pion mass, corrected with the one-loop factor Y . Figure provided by JLQCD (Ishizuka et al. (1997)).

the University of Leiden for hospitality while preparing this talk. This work was supported in part by the US Department of Energy through an Outstanding Junior Investigator grant.

References

- C. Bernard and M. Golterman, Phys. Rev. **D46** (1992) 853.
- C. Bernard and M. Golterman, Nucl. Phys. **B** (Proc. Suppl.) **30** (1993) 217.
- C. Bernard and M. Golterman, Phys. Rev. **D49** (1994) 486.
- C. Bernard and M. Golterman, Phys. Rev. **D53** (1996) 476.
- C. Bernard and A. Soni, Nucl. Phys. **B** (Proc. Suppl.) **9** (1989) 155.
- T. Bhattacharya and R. Gupta, Phys. Rev. **D54** (1996) 1155.
- J. Bijnens, H. Sonoda and M. Wise, Phys. Rev. Lett. **53** (1984) 2367.
- M. Booth, Phys. Rev. **D51** (1995) 2338; hep-ph/9412228.
- M. Booth et al., Phys. Rev. **D55** (1997) 3092.
- G. Chiladze, hep-ph/9704426.
- C.-K. Chow and S.-J. Rey, hep-ph/9708432.

- G. Colangelo and E. Pallante, hep-lat/9702019; hep-lat/9708005.
B. DeWitt, *Supermanifolds*, Cambridge University Press (1984).
J. Donoghue, E. Golowich and B. Holstein, Phys. Lett. **B119** (1982) 412.
J. Gasser, these proceedings.
J. Gasser and H. Leutwyler, Nucl. Phys. **B250**, 465 (1985).
J. Gasser and H. Leutwyler, Phys. Lett, **B184** (1987) 83.
M.B. Gavela et al., Nucl. Phys. **B306** (1988) 677.
M. Golterman, Acta Phys. Pol. **25** (1994) 1731.
M. Golterman and K.-C. Leung, Phys. Rev. **D56** (1997) 2950.
S. Gottlieb, Nucl. Phys. **B** (Proc. Suppl.) **53** (1997) 155.
M. Guagnelli, E. Marinari and G. Parisi, Phys. Lett. **B240** (1990) 188.
R. Gupta et al., Nucl. Phys. **B383** (1992) 309; Phys. Rev. **D48** (1993) 388.
H. Hamber and G. Parisi, Phys. Rev. Lett. **47** (1981) 1792; E. Marinari, G. Parisi and C. Rebbi, Phys. Rev. Lett. **47** (1981) 1795.
N. Ishizuka, for JLQCD, to be published in the Proceedings of the XVth International Conference on Lattice Field Theory, Edinburgh, Scotland (1997).
J. Kambor, J. Missimer and D. Wyler, Nucl. Phys. **B346** (1990) 17.
M. Kim and S. Kim, hep-lat/9608091.
Y. Kuramashi et al., Phys. Rev. Lett. **71** (1993) 2387; Phys. Rev. **D52** (1995) 3003.
J. Labrenz and S. Sharpe, Phys. Rev. **D54** (1996) 4595.
M. Lüscher, Comm. Math. Phys. **105** (1986) 153; Nucl. Phys. **B354** (1991) 531.
A. Morel, J. Physique **48** (1987) 111.
S. Sharpe, Phys. Rev. **D41** (1990) 3223; S. Sharpe, Nucl. Phys. **B** (Proc. Suppl.) **17** (1990) 146; G. Kilcup et al., Phys. Rev. Lett. **64** (1990) 25.
S. Sharpe, Phys. Rev. **D46** (1992) 3146.
S. Sharpe, Nucl. Phys. **B** (Proc. Suppl.) **53** (1997) 181.
S. Sharpe, hep-lat/9707018.
S. Sharpe and Y. Zhang, Phys. Rev. **D53** (1996) 5125.
G. Veneziano, Nucl. Phys. **B159** (1979) 213.
S. Weinberg, Physica **96A**, 327 (1979).
D. Weingarten, Phys. Lett. **B109** (1982) 57.
E. Witten, Nucl. Phys. **B159** (1979) 269.
T. Yoshie, to be published in the Proceedings of the XVth International Conference on Lattice Field Theory, Edinburgh, Scotland (1997) (hep-lat/9711017).